Statistica Sinica Preprint No: SS-2026-0100	
Title	Non-stationary Covariance Functions for Spatial Data on Linear Networks
Manuscript ID	SS-2026-0100
URL	http://www.stat.sinica.edu.tw/statistica/
DOI	10.5705/ss.202026.0100
Complete List of Authors	Alfredo Alegria
Corresponding Authors	Alfredo Alegria
E-mails	alfredo.alegria@uc.cl
Notice: Accepted author version.	

Statistica Sinica: Newly accepted Paper

Statistica Sinica

NON-STATIONARY COVARIANCE FUNCTIONS FOR SPATIAL DATA ON LINEAR NETWORKS

Alfredo Alegría

Department of Statistics, Pontificia Universidad Católica de Chile, Santiago, Chile

Abstract: We introduce a novel class of non-stationary covariance functions for random fields on linear networks that allows both the variance and the correlation range of the random field to vary spatially. The proposed covariance functions are useful to model random fields with a spatial dependence that is locally isotropic with respect to the resistance metric, a distance that reflects the topology of the network. We assess the statistical and computational performance of a weighted local likelihood estimator for the proposed models using synthetic data generated on the street network of the University of Chicago neighborhood. The framework also admits explicit stochastic representations of the associated random fields, as well as an extension to matrix-valued covariance functions for vector-valued random fields.

Key words and phrases: Generalized Stieltjes functions, Laplacian matrix, Log Gaussian Cox process, Positive definite functions, Gaussian random field, Resistance metric, Vector-valued random field, Weighted local likelihood

Statistica Sinica: Newly accepted Paper

1. Introduction

Data indexed by locations on a network arise naturally in a variety of applications, such as processes on road, river, and electrical networks. Recent developments in the theory and methodology of spatial statistics on linear networks can be found in Baddeley et al. (2017), Anderes et al. (2020), Cronie et al. (2020), Moradi and Mateu (2020), Baddeley et al. (2021), Porcu et al. (2023), Bolin et al. (2024), Møller and Rasmussen (2024), Moradi and Sharifi (2024), Filosi et al. (2025), González-Pérez et al. (2025), Bolin et al. (2025), Alegría et al. (2026) and Filosi et al. (2027).

Specifically, a linear network $\mathcal{L}$ is the union $\mathcal{L} = \bigcup_{i=1}^{m} \ell_i$ of closed line segments $\ell_1, \ldots, \ell_m$ in $\mathbb{R}^2$, with $m < \infty$. Each segment has positive finite length and intersects other segments only at endpoints. Throughout, the network is assumed to be path-connected.

A second-order Gaussian random field (GRF), namely $\{X(s) : s \in \mathcal{L}\}$, is completely characterized by its mean function, which we assume to be zero for simplicity, and by its covariance function, given by $K(s,t) = \mathrm{cov}[X(s), X(t)]$, $s, t \in \mathcal{L}$. The construction of valid and versatile covariance functions is challenging because of the requirement that the covariance

matrix of $(X(s_1), \ldots, X(s_N))^\top$, given by

$$\boldsymbol{\Sigma} = \big[K(s_i, s_j)\big]_{i,j=1}^{N},$$

must be positive semidefinite, for all $N \in \mathbb{N}$ and for all collection of spatial locations $s_1, \ldots, s_N$ in $\mathcal{L}$. In other words, K must be a positive semidefinite function. The spectral theory of random fields on Euclidean spaces is useful to check for positive semidefiniteness of a candidate function (see, e.g., Yaglom, 1987). In the linear network setting, spectral constructions are also available, since expansions in terms of the eigenfunctions of the Laplacian yield valid covariance models, as in the Whittle–Matérn fields of Bolin et al. (2024) and Bolin et al. (2025). The eigenpairs, however, depend on the specific network and must be recomputed for each one, whereas the approach adopted here establishes positive semidefiniteness simultaneously for all networks.

It is commonly assumed that the covariance function is isotropic, meaning that there exists a function $C : [0, \infty) \to \mathbb{R}$ such that $K(s, t) = C(\mathrm{d}(s, t))$, for all $s, t \in \mathcal{L}$, with $\mathrm{d}(\cdot, \cdot)$ standing for a distance metric on $\mathcal{L}$. In practice, treating network coordinates as ordinary Euclidean coordinates can distort the proximity between locations and produce unrealistic results. To address this, Anderes et al. (2020) established positive definiteness for certain classes of isotropic covariance functions under the resistance

Statistica Sinica: Newly accepted Paper

metric (an extension of the resistance metric from electrical network theory) and showed that, under the geodesic (shortest-path) metric, these classes are valid only under restrictive assumptions on the network structure. Both the resistance and geodesic metrics, unlike the Euclidean metric, take the network topology into account.

Although isotropy is a convenient assumption, it can be overly restrictive. In geostatistical applications, there is increasing demand for more flexible models, particularly when analyzing data over large domains where the properties of the process may vary across space. See Bolin et al. (2025) for a recent development of non-stationary random fields on metric graphs formulated as solutions to stochastic partial differential equations, and an application to traffic speed data. In the context of log Gaussian Cox processes (LGCPs) (Cox, 1955), where the intensity of point occurrences is governed by a log Gaussian random field, isotropy of the underlying GRF prevents the number of points and the spatial extent of point clusters from varying across the domain. This limitation has been studied for point processes in Euclidean spaces by Dvořák et al. (2019). Similar issues arise on linear networks, as discussed by Baddeley et al. (2017), encouraging the development of more flexible models.

Motivated by this, we propose a general class of non-stationary covari-

Statistica Sinica: Newly accepted Paper

ance functions on linear networks, that is, covariance functions not solely determined by distance. The proposed covariance models allow both the variance and the correlation range of the random field to vary across the network, providing a network analogue of models previously proposed in Euclidean spaces (Paciorek, 2003; Paciorek and Schervish, 2006; Anderes and Stein, 2011; Kleiber and Nychka, 2012; Mateu et al., 2013; Liang and Marcotte, 2016). Our framework produces covariance functions that are locally isotropic with respect to the resistance metric, ensuring interpretability and alignment with the topology of the network.

We exploit the connection between the proposed covariance functions and the class of generalized Stieltjes functions (see Koumandos and Pedersen, 2019; Menegatto, 2020 for a detailed treatment) to provide examples of non-stationary covariance functions in closed form.

To address statistical inference for the proposed models, we revisit the weighted local likelihood approach, originally introduced by Anderes and Stein (2011) for Euclidean spaces, and adapt it to the network setting. We then conduct a simulation study using synthetic data generated on the street network of the University of Chicago neighborhood, in which we estimate the local correlation range, examine the behavior of the method under different weighting schemes, and evaluate its computational performance.

Statistica Sinica: Newly accepted Paper

The contributions of the paper can be summarized as follows.

(i) Theorem 1 provides a general criterion for the positive semidefiniteness of a class of non-stationary covariance functions on arbitrary linear networks; this is the central result of the paper.

(ii) The connection with generalized Stieltjes functions yields closed-form examples, and we show how the model can be calibrated to a prescribed local variance and a prescribed local correlation range.

(iii) We adapt the weighted local likelihood method to the network setting in order to estimate the proposed models, and study, by simulation, the statistical and computational behavior of two weighting schemes.

(iv) Finally, two optional extensions of the construction are collected in the Supplementary Material, a stochastic representation of the associated random fields, which is useful for the design of simulation algorithms, and a version for vector-valued GRFs on linear networks.

The paper is organized as follows. Section 2 reviews the definition and properties of the resistance metric. Section 3 presents the main theorem, examples, practical guidance on the specification of the parameter functions, and illustrations, and closes with a brief account of two extensions of the framework. Section 4 describes the weighted local likelihood method,

reports the results of the simulation study, and discusses the choice of the bandwidth. Section 5 concludes the paper with a discussion and directions for future research. A proof of the main result is given in the appendix. The Supplementary Material complements the article with the two extensions and their proofs, together with a sensitivity analysis of the estimates with respect to the bandwidth.

2. Resistance metric

This section reviews the definition and properties of the resistance metric introduced in Anderes et al. (2020), as it is essential for building the non-stationary covariance functions proposed in this work.

We begin by representing the linear network as a metric graph $(\mathcal{V}, \mathcal{E})$, where the vertex set $\mathcal{V} = \{v_1, \ldots, v_n\}$ corresponds to the endpoints of $\mathcal{L}$, and the edge set $\mathcal{E}$ corresponds to the interiors of the linear segments $\ell_1, \ldots, \ell_m$. The length of ℓ_i is denoted by $|\ell_i|$. We write $v_i \sim v_j$ if the distinct vertices v_i and v_j are connected by an edge. For any pair of vertices $v_i, v_j \in \mathcal{V}$, the conductance function is defined as

$$\operatorname{con}(v_i, v_j) = \begin{cases} 1/\|v_i - v_j\|, & \text{if } v_i \sim v_j, \\ 0, & \text{otherwise,} \end{cases}$$

where $\|\cdot\|$ denotes the Euclidean norm in $\mathbb{R}^2$, so that $\|v_i - v_j\|$ is the length

of the segment joining two adjacent vertices. Using this function, we can build a matrix $\mathbf{\Delta}$ indexed by the vertices in $\mathcal{V}$, with entries

$$\mathbf{\Delta}(v_i, v_j) = \begin{cases} 1 + c(v^*), & \text{if } v_i = v_j = v^*, \\ c(v_i), & \text{if } v_i = v_j \neq v^*, \\ -\text{con}(v_i, v_j), & \text{otherwise,} \end{cases}$$

where $v^* \in \mathcal{V}$ is an arbitrary reference vertex and $c(v_i) = \sum_{v \sim v_i} \text{con}(v_i, v)$. The resulting matrix can be viewed as a modification of the graph Laplacian, where the inclusion of an additional unit term on the diagonal guarantees strict positive definiteness. This construction is invariant to the choice of v^* (Anderes et al., 2020).

To define the resistance metric, we introduce an auxiliary GRF on $\mathcal{L}$, given by

$$A(s) = A_0(s) + \sum_{i=1}^{m} A_i(s), \qquad s \in \mathcal{L}, \tag{2.1}$$

where $A_0, \ldots, A_m$ are independent GRFs defined as follows:

- The base component A_0 is first defined on the vertices as a multivariate normal vector:

  $$(A_0(v_1), \ldots, A_0(v_n))^\top \sim \mathcal{N}_n\big(\mathbf{0}, \mathbf{\Delta}^{-1}\big).$$

  Next, A_0 is extended from the vertices to the edges using linear interpolation.

- For $i = 1, \ldots, m$,

$$A_i(s) = \begin{cases} B_i(s), & \text{for } s \in \ell_i, \\ 0, & \text{for } s \in \mathcal{L} \setminus \ell_i, \end{cases}$$

  where $B_1, \ldots, B_m$ are independent standard Brownian bridges, each defined on an interval of length $|\ell_i|$, starting and ending at zero, and independent of A_0. Since each B_i is defined on an interval, writing $B_i(s)$ implicitly identifies points s along ℓ_i with points in this interval via arc length parameterization.

For additional details on the construction of the auxiliary GRF, we refer the reader to Anderes et al. (2020) and Møller and Rasmussen (2024).

The resistance metric on $\mathcal{L}$ can now be defined as the variogram of the auxiliary GRF in Equation (2.1), that is,

$$\mathrm{d}_R(s,t) = \mathrm{var}[A(s) - A(t)], \qquad s,t \in \mathcal{L}. \tag{2.2}$$

This metric extends the classical resistance metric from electrical network theory (Klein and Randić, 1993), originally defined on the vertex set, to the continuum of points along the edges of the graph. When evaluated on any additional points along the edges, d_R coincides with the metric obtained from the corresponding discrete electrical network. Interestingly, the resistance and geodesic distances coincide when $\mathcal{L}$ is a tree, that is,

a connected graph with no cycles. Møller and Rasmussen (2024) provide more fully developed algebraic expressions for the resistance metric, which facilitate its implementation.

We turn to a description of the range of isotropic covariance functions attainable using the resistance metric. A function $\varphi : [0, \infty) \to \mathbb{R}$ is said to be completely monotone on $[0, \infty)$ if it is continuous on $[0, \infty)$, infinitely differentiable on $(0, \infty)$, and satisfies $(-1)^j \varphi^{(j)}(z) \geq 0$, $z > 0$, for every integer $j \geq 0$, where $\varphi^{(j)}$ denotes the j-th derivative of φ and $\varphi^{(0)} = \varphi$. Anderes et al. (2020) showed that for any completely monotone function φ, the function $K(s,t) = \varphi\big(\mathrm{d}_R(s,t)\big)$ is (strictly) positive definite on $\mathcal{L} \times \mathcal{L}$. As a consequence, many popular parametric classes of covariance functions developed for Euclidean spaces are also valid with respect to the resistance metric for general linear networks (see Anderes et al., 2020, Table 1).

In contrast, the geodesic distance provides a more restrictive alternative. For example, if $\mathcal{L}$ contains three distinct paths connecting two points $s, t \in \mathcal{L}$, the classical exponential covariance function, defined with respect to the geodesic metric, is no longer positive definite on this network (Anderes et al., 2020). Consequently, covariance functions defined in terms of completely monotone functions, which are mixtures of exponential covariance functions, are no longer positive definite on such networks when the

geodesic metric is used. This considerably restricts the use of the geodesic distance, as many real situations, such as phenomena on street networks, typically do not satisfy this condition.

Møller and Rasmussen (2024) also emphasize, in the context of point processes on linear networks, the advantages of the resistance metric over the geodesic metric in terms of flexibility. In particular, the use of d_R allows one to model stronger clustering effects in Cox processes and higher degree of repulsiveness in determinantal point processes.

3. Non-stationary covariance functions

3.1 Main result

We now present a general theorem for constructing non-stationary families of covariance functions on linear networks.

Theorem 1. *Let $a : \mathcal{L} \to (0, \infty)$ and $b : \mathcal{L} \to (0, \infty)$, and define $\alpha(s, t) = [a(s) + a(t)]/2$. Let $d_R(s, t)$ be the resistance metric between s and t, and let F denote a positive finite measure on $(0, \infty)$. Then, the function*

$$K(s,t) = \int_0^\infty \frac{\sqrt{b(s)b(t)}}{\sqrt{\alpha(s,t) + d_R(s,t)w}} dF(w), \qquad s, t \in \mathcal{L}, \tag{3.3}$$

is positive semidefinite on $\mathcal{L} \times \mathcal{L}$.

Our proof of Theorem 1, presented in the appendix, adapts ideas in-

Statistica Sinica: Newly accepted Paper

troduced in Paciorek (2003) for establishing positive definiteness of non-stationary covariance functions in Euclidean spaces. To the best of our knowledge, the present work is the first to extend this approach to linear networks. The fact that the resistance metric is defined as the variogram of a specific auxiliary GRF gives the proof a distinctive character.

Remark 1. Theorem 1 does not require the edges of $\mathcal{L}$ to be line segments. The only property of d_R used in the proof is that it is the variogram of the auxiliary GRF of Equation (2.1). Hence the result remains valid for a network $\mathcal{L} = \bigcup_{i=1}^{m} \gamma_i$ whose edges are curves $\gamma_i : [0,1] \to \mathbb{R}^2$ of finite length, provided that the auxiliary GRF is built from the associated metric graph, with the conductances defined through the lengths $|\gamma_i|$ instead of the Euclidean distances between adjacent vertices. This is the setting of graphs with Euclidean edges of Anderes et al. (2020). We restrict the exposition to unions of line segments only for consistency with the standard definition of a linear network and with the networks used in our examples.

Observe that if s and t are near a fixed location $s_0 \in \mathcal{L}$, and both functions b and a are sufficiently smooth, then

$$K(s,t) \approx \int_0^\infty \frac{b(s_0)}{\sqrt{a(s_0) + \mathrm{d}_R(s,t)w}} \mathrm{d}F(w).$$

Statistica Sinica: Newly accepted Paper

In other words, $K(s,t)$ depends approximately only on the resistance metric $\mathrm{d}_R(s,t)$. This property allows us to construct covariance models with locally isotropic behavior with respect to d_R, reflecting the topology of the linear network.

In this framework, the function b provides a way to modulate the locally varying variance of the random field, while the function a regulates how quickly the covariance function decreases with distance. In particular, a can be adjusted to influence the locally adaptive correlation range (the distance beyond which correlations fall below 0.05). Neither b nor a is, however, the local variance or the local correlation range itself; Section 3.3 makes the correspondence explicit.

The positivity of a and b is the only condition used in the proof of Theorem 1. Regularity is nevertheless relevant to the local isotropy just described. Continuity with respect to d_R, in the sense that $a(s) \to a(s_0)$ and $b(s) \to b(s_0)$ as $\mathrm{d}_R(s,s_0) \to 0$, makes the approximation above exact as s and t approach s_0, and it also gives a continuous K and a mean-square continuous random field, since $\mathrm{E}\big[\{X(s)-X(t)\}^2\big] \to 0$ as $\mathrm{d}_R(s,t) \to 0$. For the approximation to be useful over a window of positive radius, however, a and b must be nearly constant on that window, which a Lipschitz condition with respect to d_R quantifies, the error being then of the order

Statistica Sinica: Newly accepted Paper

of the radius times their Lipschitz constants. The smaller the Lipschitz constants of a and b, the larger the window over which the field can be treated as isotropic, which is the property that the weighted local likelihood method of Section 4 relies on. In the Euclidean setting, conditions of this kind appear in asymptotic analyses, imposed there on higher derivatives of the covariance (Kleiber and Nychka, 2012), and in locally stationary time series they are imposed on the time-varying spectral representation (Dahlhaus, 1997). Beyond this, since ψ is smooth on $(0, \infty)$ and K is obtained from a, b and d_R by composition, away from the diagonal K inherits the regularity of a and b, as do the local variance and the local correlation range.

3.2 Examples

A direct calculation shows that the covariance function in Equation (3.3) admits the following representation:

$$K(s,t) = \begin{cases} \dfrac{b(s)}{\sqrt{a(s)}} F((0,\infty)), & \text{if } s = t, \\ \sqrt{\dfrac{b(s)b(t)}{\mathrm{d}_R(s,t)}}\, \psi\left(\dfrac{\alpha(s,t)}{\mathrm{d}_R(s,t)}\right), & \text{if } s \neq t, \end{cases}$$

Statistica Sinica: Newly accepted Paper

where

$$\psi(r) = \int_0^\infty \frac{1}{\sqrt{r+w}} \mathrm{d}F(w), \qquad r > 0. \tag{3.4}$$

Functions of the form (3.4) belong to the class of generalized Stieltjes functions of order 1/2 (see, e.g., Koumandos and Pedersen, 2019). When a and b are constant functions, we recover a subclass of the isotropic covariance functions presented in Anderes et al. (2020), since every generalized Stieltjes function is completely monotone (see, e.g., Menegatto, 2020, Section 2.2).

Since closed-form expressions for generalized Stieltjes functions are available in standard tables of integral transforms such as (Erdélyi, 1954, Chapter 14), it is straightforward to derive explicit examples of non-stationary covariance functions.

Example 1. Let F be the Dirac delta measure at $\eta > 0$, that is, $\mathrm{d}F(w) = \mathrm{d}\delta_\eta(w)$. Then, we immediately obtain the covariance function

$$K(s,t) = \sqrt{\frac{b(s)b(t)}{\alpha(s,t)}} \left(1 + \frac{\eta \mathrm{d}_R(s,t)}{\alpha(s,t)}\right)^{-1/2}. \tag{3.5}$$

Example 2. Let $\mathrm{d}F(w) = (1/\eta)\exp(-w/\eta)\mathrm{d}w$, for $\eta > 0$. Equation 14.4.10 in Erdélyi (1954) gives the associated generalized Stieltjes function,

Statistica Sinica: Newly accepted Paper

$\psi(r) = \sqrt{\pi/\eta}\,\exp(r/\eta)\,\mathrm{erfc}(\sqrt{r/\eta})$, and therefore

$$K(s,t) = \begin{cases} \dfrac{b(s)}{\sqrt{a(s)}}, & \text{if } s = t, \\ \sqrt{\dfrac{\pi b(s) b(t)}{\eta\, \mathrm{d}_R(s,t)}}\, \exp\left(\dfrac{\alpha(s,t)}{\eta \mathrm{d}_R(s,t)}\right) \mathrm{erfc}\left(\sqrt{\dfrac{\alpha(s,t)}{\eta \mathrm{d}_R(s,t)}}\right), & \text{if } s \neq t, \end{cases}$$

where erfc denotes the complementary error function.

Example 3. Let $\mathrm{d}F(w) = \sqrt{\eta}\pi^{-1} w^{-1/2} (\eta + w)^{-1} \mathrm{d}w$, for $\eta > 0$, a scaled Beta prime probability measure. Equation 14.4.9 in Erdélyi (1954) gives $\psi(r) = (2/\pi)\eta^{-1/2}\, {}_2F_1(1, 1/2, 3/2; 1 - r/\eta)$, where ${}_2F_1$ denotes the Gauss hypergeometric function, so that

$$K(s,t) = \begin{cases} \dfrac{b(s)}{\sqrt{a(s)}}, & \text{if } s = t, \\ \dfrac{2}{\pi} \sqrt{\dfrac{b(s) b(t)}{\eta\, \mathrm{d}_R(s,t)}}\, {}_2F_1\left(1, 1/2, 3/2; 1 - \dfrac{\alpha(s,t)}{\eta \mathrm{d}_R(s,t)}\right), & \text{if } s \neq t. \end{cases}$$

3.3 Parameterization

We now show how to choose the functions a and b so that the random field has a prescribed local variance and a prescribed local correlation range. Since $\mathrm{var}[X(s)] = K(s,s) = b(s) F((0,\infty))/\sqrt{a(s)}$, a target local variance

Statistica Sinica: Newly accepted Paper

$c : \mathcal{L} \to (0, \infty)$ is attained with

$$b(s) = \frac{c(s)\sqrt{a(s)}}{F((0,\infty))}, \qquad s \in \mathcal{L}, \tag{3.6}$$

so that b is not the local variance itself but a rescaled version of it. The same distinction arises in Euclidean non-stationary models of the Paciorek type (Kleiber and Nychka, 2012, Section 2).

Fix $s_0 \in \mathcal{L}$ and consider locations s and t near s_0. The local correlation function is

$$\rho(\mathrm{d}_R(s,t)) = \frac{\sqrt{u}\,\psi(u)}{F((0,\infty))}, \qquad u = \frac{a(s_0)}{\mathrm{d}_R(s,t)}, \tag{3.7}$$

with ψ as in Equation (3.4), and it is decreasing in $\mathrm{d}_R(s,t)$. It depends on $\mathrm{d}_R(s,t)$ and $a(s_0)$ only through their ratio, so that the distance at which it falls below 0.05, which we call the local correlation range at s_0 and denote by $r(s_0)$, is a constant multiple of $a(s_0)$, the constant depending on F only. Since s_0 is arbitrary, the same holds at every location of the network. For the covariance function (3.5) the constant is explicit, since inverting its local correlation function at the level 0.05 gives $r(s) = 399\,a(s)/\eta$, the size of the constant reflecting the slow decay of this correlation function.

3.4 Illustration

To illustrate our proposal, we simulate a GRF on a linear network formed by the mortar lines of a brick wall. This network, consisting of 156 vertices

Statistica Sinica: Newly accepted Paper

and 203 edges, and available in the `R` package `spatstat` (Baddeley and Turner, 2005), has been the focus of studies on the positions of spider webs of the urban wall spider Oecobius navus (Voss et al., 2007).

We use the covariance function in Equation (3.5) with $\eta = 1$ and the parameterization $b(s) = c(s)\sqrt{a(s)}$, for some function $c : \mathcal{L} \to (0, \infty)$, which ensures that $\text{var}[X(s)] = K(s, s) = c(s)$, for all $s \in \mathcal{L}$. Specifically, we consider

$$a(s) = 2500 \times \exp\left(-\frac{\mathrm{d}_R(s, s^*)}{100}\right), \qquad s \in \mathcal{L}, \tag{3.8}$$

and

$$c(s) = 2 \times \exp\left(-\frac{\mathrm{d}_R(s, s^*)}{1000}\right), \qquad s \in \mathcal{L}, \tag{3.9}$$

where s^* is a fixed point on $\mathcal{L}$. Both functions attain their maximum at s^* and decay exponentially as s moves away from this point, as illustrated in Figure 1. Accordingly, we expect the simulated GRF to exhibit larger correlation range and higher variance at locations near s^*, decreasing as one moves away from this point.

To better illustrate the local behavior of this covariance function, Figure 2 shows the curves

$$\mathrm{d}_R \mapsto \frac{\sqrt{a_0}}{\sqrt{a_0 + \mathrm{d}_R}}$$

for different values of a_0. These curves capture part of the local isotropic

Statistica Sinica: Newly accepted Paper

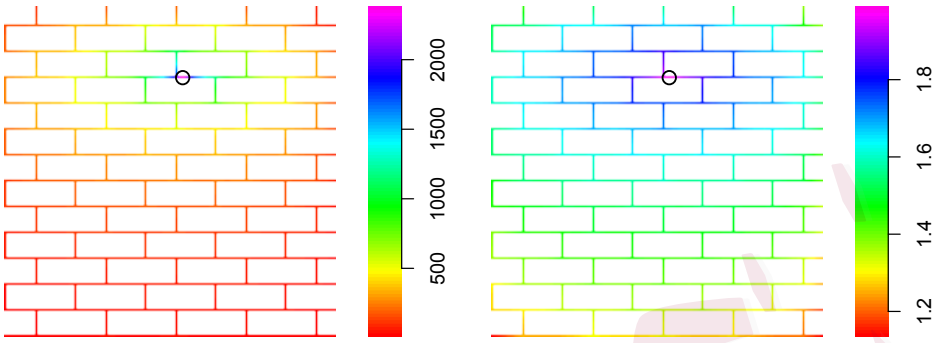


Figure 1: Functions a (left) and c (right), defined in Equations (3.8) and (3.9), respectively, on the `spiders` linear network. The circle indicates the point $s^* \in \mathcal{L}$ involved in the definitions of a and c.

correlation structures that the non-stationary covariance function exhibits. They are displayed over the interval $(0, 800)$ since the maximum resistance distance between two points in this domain is approximately 837.

Figure 3 (left panel) shows the simulated GRF over 5,684 sites (28 per edge). The simulated field attains high values at sites in the top part of the linear network, and because the correlation range is greater in this region, these high values extend over a wide area. In contrast, at sites in the lower part of the linear network, the simulated field varies more rapidly, reflecting a smaller correlation range.

Statistica Sinica: Newly accepted Paper

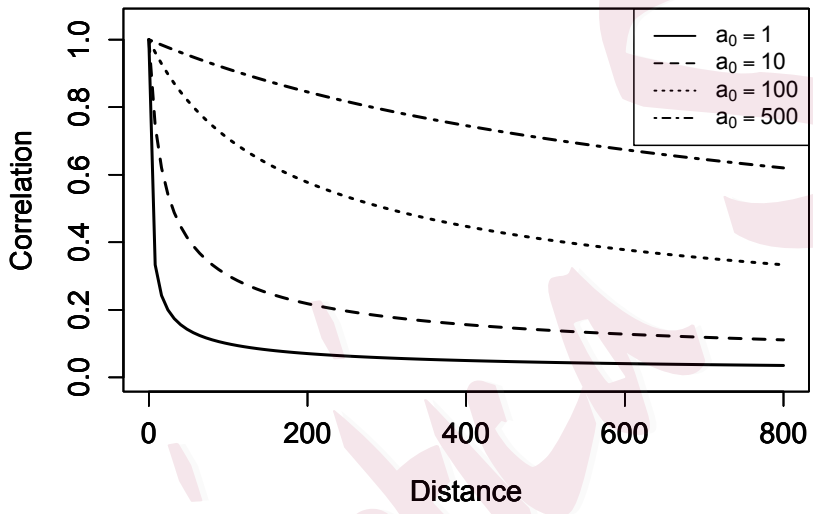


Figure 2: Mapping $\mathrm{d}_R \mapsto \sqrt{a_0}/\sqrt{a_0 + \mathrm{d}_R}$ for selected values of a_0, illustrating how the local isotropic correlation structure of the non-stationary covariance function (3.5) depends on a_0.

Statistica Sinica: Newly accepted Paper

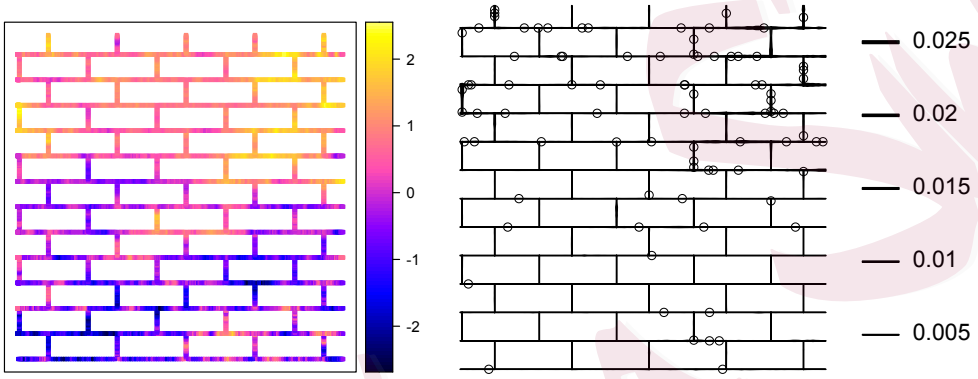


Figure 3: (Left) Simulated zero-mean GRF on the `spiders` linear network, with the non-stationary covariance function given in Equation (3.5); the color scale gives the value of $X(s)$ at the $5,684$ simulated sites. (Right) Corresponding realization of a LGCP, with the points of the process superimposed on the network and line thickness proportional to the intensity $\Lambda(s) = 0.002 \times \exp\{X(s)\}$, whose values are reported in the legend.

Statistica Sinica: Newly accepted Paper

The right panel of Figure 3 shows the realization of the corresponding LGCP, where the log Gaussian random field is defined as $\Lambda(s) = 0.002 \times \exp\{X(s)\}$, with $X(s)$ denoting the underlying GRF. Recall that, conditioned on Λ, this point process on $\mathcal{L}$ is almost surely a Poisson process with intensity function Λ (with respect to the arc length measure on $\mathcal{L}$). As expected, more points occur in the upper part of the network, covering a larger area, while fewer points are present in the lower part. For a more detailed treatment of Cox processes on linear networks, we refer the reader to Møller and Rasmussen (2024).

3.5 Two extensions

We close this section by mentioning two extensions of the construction, both of which follow from the representation obtained in the proof of Theorem 1 and are developed in the Supplementary Material. Section S1 provides an explicit stochastic representation of a random field with covariance function (3.3) (Theorem S1), which is of interest for the design of simulation algorithms that avoid the cubic cost of the Cholesky decomposition. Section S2 extends Theorem 1 to matrix-valued covariance functions for vector-valued GRFs on linear networks (Theorem S2), the network counterpart of a result

Statistica Sinica: Newly accepted Paper

of Kleiber and Nychka (2012) for Euclidean spaces, and complements the isotropic matrix-valued models on trees of Filosi et al. (2025). Both extensions are self-contained, so the reader interested only in the estimation problem may proceed directly to Section 4.

4. Weighted local likelihood

4.1 Description of the method

We consider the weighted local likelihood estimation proposed by Anderes and Stein (2011). We now describe the method and the necessary modifications required to adapt it to the network context.

Let $X(s_1)\ldots, X(s_N)$ be a realization of a GRF on $\mathcal{L}$. For any given site $s \in \mathcal{L}$, let $\mathcal{N}_{s,k}$ denote the set of k observations nearest to s with respect to the resistance metric. Recall that our goal is to estimate a and b at the selected site s. Given weights $\lambda_1, \ldots, \lambda_N$, the weighted local likelihood function is defined as

$$\mathcal{W}\big(a_0, b_0 \mid X(s_1), \ldots, X(s_N)\big) = \sum_{k=1}^{N} \lambda_k \big[\mathrm{Lik}(a_0, b_0 \mid \mathcal{N}_{s,k}) - \mathrm{Lik}(a_0, b_0 \mid \mathcal{N}_{s,k-1})\big],$$

where $\mathrm{Lik}(a_0, b_0 \mid \mathcal{N}_{s,k})$ denotes the log-likelihood of the data in $\mathcal{N}_{s,k}$, with a_0 and b_0 representing fixed values of the functions $a(\cdot)$ and $b(\cdot)$. As in Anderes and Stein (2011), we define $\mathrm{Lik}(a_0, b_0 \mid \mathcal{N}_{s,0})$ as 0.

Statistica Sinica: Newly accepted Paper

The local estimate of $(a(s), b(s))$ is given by

$$\big(\hat{a}(s), \hat{b}(s)\big) = \arg\max_{(a_0,b_0)} \mathcal{W}\big(a_0, b_0 \mid X(s_1), \ldots, X(s_N)\big).$$

The principle behind this method is that we locally fit an isotropic model, not simply by taking a window of data around s (a strategy also used in Anderes and Stein, 2011, which has been shown to be less competitive), but by considering inflating neighborhoods and gradually assigning less weight to those that cover a very large region. For this reason, the weights include a bandwidth parameter to control this effect.

4.2 Simulation

In our simulation experiments, we focus on two main aspects. First, we study the performance of the weighted local likelihood method in the linear network setting, where it has not been previously examined. Second, we evaluate both the statistical and computational performance of compactly supported weights λ_k^{cs} in comparison with Gaussian weights λ_k^{g}.

Specifically, we consider the following weighting schemes:

$$\lambda_k^{\mathrm{cs}} = \left(1 - \frac{\mathrm{d}_R(s, s_k)}{\tau}\right)_+, \qquad k = 1, \ldots, N, \tag{4.10}$$

where $(r)_+ = \max\{0, r\}$ denotes the positive part function, and

$$\lambda_k^{\mathrm{g}} = \exp\left(-\frac{\mathrm{d}_R(s, s_k)^2}{\eta^2}\right), \qquad k = 1, \ldots, N, \tag{4.11}$$

Statistica Sinica: Newly accepted Paper

where we assume that the sites $s_1, \ldots, s_N$ are ordered by their distance to s, for simplicity. Here, τ and η are bandwidth parameters. Because compactly supported weights vanish beyond a certain distance when the bandwidth is moderate, only a subset of the neighborhoods $\mathcal{N}_{s,1}, \ldots, \mathcal{N}_{s,N}$ may contribute to the local likelihood at s, which can reduce the computational cost.

We consider the `Chicago` street network available in the `R` package `spatstat`, and the covariance function in Equation (3.5), with the parameterization discussed in Section 3.4. Following Anderes and Stein (2011), we assume for simplicity that the variance of the random field is known and equal to one, so that we focus on the estimation of the local practical range. The function a used in our study is shown in the top panel of Figure 4. We also highlight six randomly selected locations on the network at which a will be estimated.

We simulate 100 independent realizations of the GRF on this domain at 503 locations (one at the midpoint of each edge). For each realization, we estimate a at the six selected sites. The weighted local likelihood method is implemented with the weighting schemes described above. We use bandwidth parameters $\eta = 120$ and $\tau = 200$, which produce weight functions with a comparable spatial extent but distinct structural features (see the bottom panel of Figure 4). For reference, the maximum resistance distance

Statistica Sinica: Newly accepted Paper

between two points in this network is approximately 675.

In Figure 5, we show the centered boxplots of the estimates across the 100 realizations, for each weighting scheme and each of the six selected sites. Overall, no significant bias is observed in any of the boxplots, demonstrating the effectiveness of the method. One point of interest is the higher variance in the estimates at site 2. This effect is consistent with the site's proximity to the boundary of the network, which reduces the number of neighbors that effectively contributes to the local estimate. A similar observation was reported by Anderes and Stein (2011).

Next, we comment on the comparison between the two types of weights. We observe similar results for both approaches, with a slight advantage for the compactly supported weights in terms of variance at sites 4, 5, and 6. However, at the boundary site 2, the variance is more pronounced when using compactly supported weights. Overall, compactly supported weights appear to be competitive from a statistical perspective.

We also compare the computational performance of the weighting schemes by measuring evaluation times as a function of the sample size of the GRF. Specifically, we simulate GRFs with $N = 503, 1006, 1509$, and 2012, which correspond to taking 1, 2, 3, and 4 locations per edge, respectively, and implement the method using compactly supported weights with bandwidth

Statistica Sinica: Newly accepted Paper

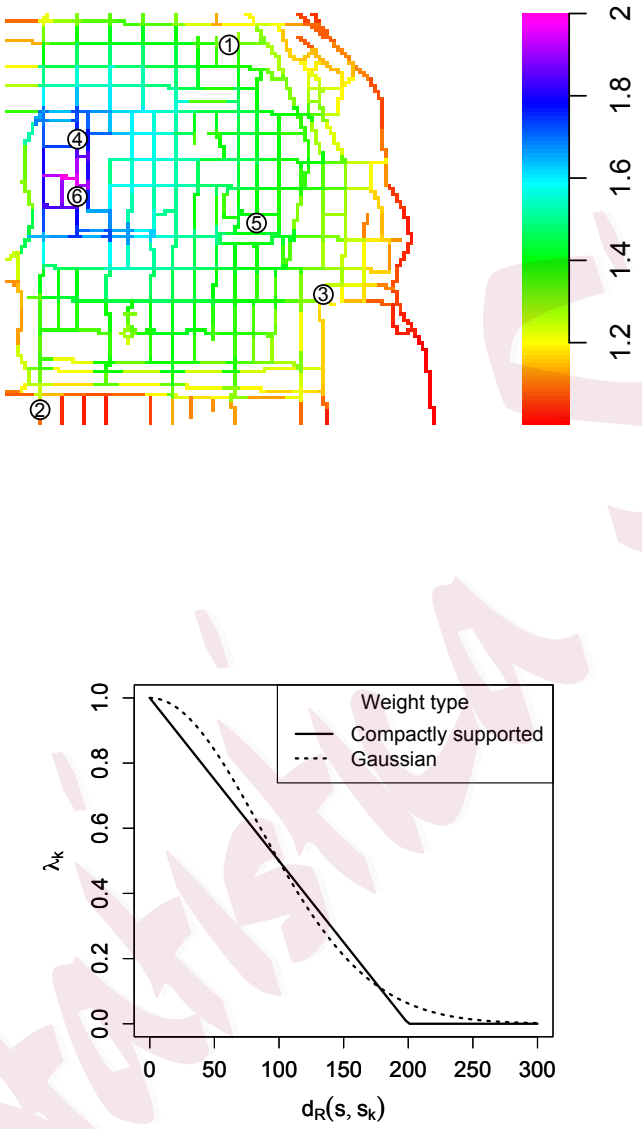


Figure 4: (Top) The function a used in our simulations on the `Chicago` street network. Six randomly selected locations where a will be estimated are highlighted. (Bottom) Decay of the weights as a function of the resistance metric for the compactly supported ($\tau = 200$) and Gaussian ($\eta = 120$) weighting schemes.

Statistica Sinica: Newly accepted Paper

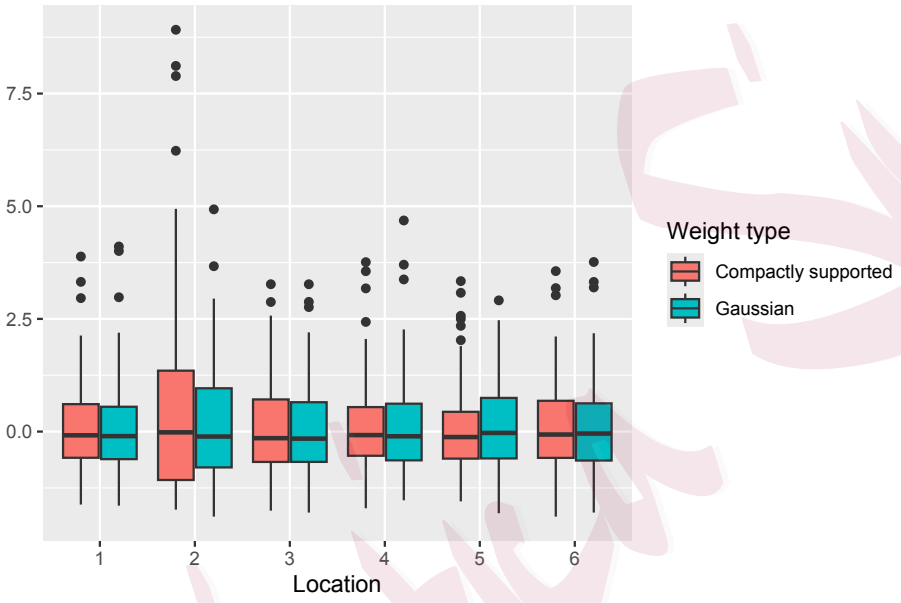


Figure 5: Centered boxplots of the estimates of a, at the six selected sites, across 100 independent realizations of a GRF with covariance function (3.5). Results are shown for the compactly supported and Gaussian weighting schemes.

Statistica Sinica: Newly accepted Paper

parameters $\tau = 100, 150$, and 200. For each configuration, we report the time required for a single evaluation of the weighted local likelihood function.

The results are summarized in Table 1, allowing us to assess the computational gains relative to the Gaussian weighting scheme. For $\tau = 100$ and 150, the reduction in computation time is particularly pronounced. For instance, when $\tau = 150$, the computation time is reduced by approximately 50% compared with Gaussian weighting scheme, whereas for $\tau = 100$, evaluating the objective function takes at most 2% of the time required with Gaussian weights, and for most sample sizes the percentage is even lower.

Our findings both support the observations reported in Anderes and Stein (2011) regarding reduced precision near the domain boundaries and provide additional insights into the statistical and computational performance of different weighting schemes. A promising strategy is to use a combination of weights, employing compactly supported weights in the interior and adapting the weights near the boundaries.

4.3 On the choice of the bandwidth

In the experiments above the bandwidths were fixed so that the two weight-

Statistica Sinica: Newly accepted Paper

Table 1: Times (in seconds) for a single evaluation of the weighted local likelihood function under each weighting scheme, as a function of the sample size N. For the compactly supported weights we consider $\tau = 100, 150$, and 200. The simulation was performed on an Apple M1 chip with 8GB of memory.

	$N = 503$	$N = 1006$	$N = 1509$	$N = 2012$
Compactly supported ($\tau = 100$)	0.046	0.322	1.348	5.037
Compactly supported ($\tau = 150$)	1.056	20.39	107.8	372.7
Compactly supported ($\tau = 200$)	2.009	35.41	196.7	648.6
Gaussian	2.257	41.35	225.8	759.0

Statistica Sinica: Newly accepted Paper

ing schemes have a comparable spatial extent, which is what makes the comparison between them meaningful. The bandwidth governs the usual trade-off between bias and variance. Section S3 of the Supplementary Material reports a sensitivity analysis of the estimates of a with respect to the bandwidth, at an interior site and at a site near the boundary of the network. Over the range of bandwidths examined the accuracy of the estimates changes by at most 2% at the interior site and by at most 15% at the site near the boundary, where fewer observations contribute.

Regarding data-driven selection, Anderes and Stein (2011) observe that classical methods such as cross-validation may fail when the data consist of a single realization of a non-stationary random field, since the observations are highly correlated and a leave-out prediction becomes unreliable. They propose alternative criteria, which remain valid in the network setting once Euclidean distances are replaced by resistance distances. A systematic study of these selectors on linear networks is beyond the scope of the present paper, and we refer the reader to Anderes and Stein (2011) for a comprehensive treatment of weights and bandwidth selection.

Statistica Sinica: Newly accepted Paper

5. Discussion

This paper proposes non-stationary covariance functions for random fields defined on linear networks. The models exhibit local isotropy with respect to the resistance metric, allowing both the variance and correlation range to vary spatially. We demonstrate the effectiveness of a weighted local likelihood approach with compactly supported weights for estimating the proposed covariance models, which provide a balance between computational efficiency and statistical accuracy. We also provide, in the Supplementary Material, a useful stochastic representation for these random fields and extend the covariance functions from the scalar to the matrix-valued setting, enabling the modeling of vector-valued random fields.

Although constructive criticism has been raised regarding covariance functions based on the resistance metric (Bolin et al., 2024), primarily because existing covariance families under this metric do not provide explicit control over the mean-square differentiability of the random field (that is, there is no direct analogue of the Matérn family of covariance functions under the resistance metric), we argue that the models introduced in this work offer considerable potential for practical applications. In the context of point process modeling, and in particular for LGCPs, local flexibility in variance and correlation range is essential for capturing heterogeneous ag-

Statistica Sinica: Newly accepted Paper

gregation structures, even when the smoothness level of the latent GRF is kept fixed (Dvořák et al., 2019). The proposed covariance models are also applicable to geostatistical data, such as continuous measurements along stream networks (Ver Hoef and Peterson, 2010). Since they do not allow control over the smoothness of the random field, their applicability is restricted to phenomena exhibiting relatively rough short-scale variations across space. This limitation concerns the smoothness of the sample paths, which under the resistance metric is governed by the behavior of K near the diagonal, and not the regularity of K as a function of its two arguments, which is inherited from a and b as discussed in Section 3.1. Extending the framework to include flexible smoothness represents a promising direction for future research.

Other strategies for modeling non-stationarity in Euclidean spaces, such as domain deformation or different variants of kernel convolutions of isotropic random fields, could potentially be adapted to linear networks (see Schmidt and Guttorp, 2020 and references therein). Another interesting avenue is the development of nonparametric and semiparametric estimation methods in the network setting, analogous to the approaches of Chang et al. (2010) and Kidd and Katzfuss (2022) in Euclidean spaces.

Supplementary Material

The online Supplementary Material contains three sections. Section S1 provides a stochastic representation of the random fields associated with the proposed covariance functions, and Section S2 extends the construction to matrix-valued covariance functions for vector-valued GRFs, the proofs of both results being included there. Section S3 reports a sensitivity analysis of the weighted local likelihood estimates with respect to the bandwidth.

Acknowledgement

The author is grateful to the Editor and to two anonymous reviewers for their careful reading and constructive comments. Alfredo Alegría is partially supported by the National Agency for Research and Development of Chile through grant ANID Fondecyt 1251154.

Appendix: Proof of Theorem 1

A direct calculation shows that, for all $w > 0$,

$$\begin{aligned}\frac{1}{\sqrt{\alpha(s,t)+\mathrm{d}_R(s,t)w}} &= \frac{1}{\sqrt{\alpha(s,t)}}\int_{\mathbb{R}}\exp\left\{-\frac{w\mathrm{d}_R(s,t)y^2}{2\alpha(s,t)}\right\}\frac{1}{\sqrt{2\pi}}\exp\left\{-\frac{y^2}{2}\right\}\mathrm{d}y \\ &= \frac{1}{\sqrt{\alpha(s,t)}}\mathrm{E}\left[\exp\left\{-\frac{w\mathrm{d}_R(s,t)Y^2}{2\alpha(s,t)}\right\}\right], \qquad \text{(A.1)}\end{aligned}$$

where the expectation in (A.1) is taken with respect to $Y \sim \mathcal{N}(0,1)$. Consequently, K in Equation (3.3) can be written as

$$K(s,t) = \frac{\sqrt{b(s)b(t)}}{\sqrt{\alpha(s,t)}} \int_0^\infty \mathrm{E}\left[\exp\left\{-\frac{w\mathrm{d}_R(s,t)Y^2}{2\alpha(s,t)}\right\}\right] \mathrm{d}F(w), \qquad s,t \in \mathcal{L}. \tag{A.2}$$

Let $\phi(\cdot;\mu,\sigma^2)$ denote the probability density function of a normal distribution with mean μ and variance σ^2. Using a convolution argument, we obtain

$$\int_{\mathbb{R}} \phi\left(z; \frac{A(s)}{\sqrt{2}}, \frac{a(s)}{4w}\right) \phi\left(z; \frac{A(t)}{\sqrt{2}}, \frac{a(t)}{4w}\right) \mathrm{d}z = \frac{\sqrt{w}}{\sqrt{\pi\alpha(s,t)}} \exp\left\{-\frac{w\big[A(s)-A(t)\big]^2}{2\alpha(s,t)}\right\}, \tag{A.3}$$

for every $w > 0$, with this expression conditioned on the values, $A(s)$ and $A(t)$, of the auxiliary GRF defined in Equation (2.1).

Notice that $A(s) - A(t) \sim \mathcal{N}(0, \mathrm{d}_R(s,t))$ and, consequently, $\big[A(s) - A(t)\big]/\sqrt{\mathrm{d}_R(s,t)}$ is equal in distribution to $Y \sim \mathcal{N}(0,1)$. Taking the expectation in (A.3) with respect to $(A(s), A(t))^\top$, we obtain

$$\mathrm{E}\left[\int_{\mathbb{R}} \phi\left(z; \frac{A(s)}{\sqrt{2}}, \frac{a(s)}{4w}\right) \phi\left(z; \frac{A(t)}{\sqrt{2}}, \frac{a(t)}{4w}\right) \mathrm{d}z\right] = \frac{\sqrt{w}}{\sqrt{\pi\alpha(s,t)}} \mathrm{E}\left[\exp\left\{-\frac{w\mathrm{d}_R(s,t)Y^2}{2\alpha(s,t)}\right\}\right], \tag{A.4}$$

where the right-hand side of (A.4) simplifies to an expectation with respect to $Y \sim \mathcal{N}(0,1)$. Therefore, using Equation (A.4) and Fubini's theorem, K

Statistica Sinica: Newly accepted Paper

in (A.2) can be written as

$$K(s,t) = \sqrt{\pi}\,\mathrm{E}\left[\int_0^\infty \int_{\mathbb{R}} \sqrt{b(s)b(t)}\,\phi\left(z; \frac{A(s)}{\sqrt{2}}, \frac{a(s)}{4w}\right)\phi\left(z; \frac{A(t)}{\sqrt{2}}, \frac{a(t)}{4w}\right)\mathrm{d}z\, w^{-1/2}\,\mathrm{d}F(w)\right]. \tag{A.5}$$

We can now conclude. Let $N \in \mathbb{N}$, $r_1, \ldots, r_N \in \mathbb{R}$, and $s_1, \ldots, s_N \in \mathcal{L}$. Multiplying (A.5) by $r_i r_j$ and summing over i and j, the finite double sum can be interchanged with the expectation and with both integrals, since all the terms involved are integrable, which gives

$$\sum_{i=1}^N \sum_{j=1}^N r_i r_j K(s_i, s_j) = \sqrt{\pi}\,\mathrm{E}\Bigg[\int_0^\infty \int_{\mathbb{R}} \Bigg\{\sum_{i=1}^N \sum_{j=1}^N r_i r_j \sqrt{b(s_i)b(s_j)}\,\phi\left(z; \frac{A(s_i)}{\sqrt{2}}, \frac{a(s_i)}{4w}\right) \phi\left(z; \frac{A(s_j)}{\sqrt{2}}, \frac{a(s_j)}{4w}\right)\Bigg\}\mathrm{d}z\, w^{-1/2}\,\mathrm{d}F(w)\Bigg].$$

For fixed z and w, the double sum in the integrand factorizes as the square of a single sum, which makes K positive semidefinite, that is,

$$\sum_{i=1}^N \sum_{j=1}^N r_i r_j K(s_i, s_j) = \sqrt{\pi}\,\mathrm{E}\Bigg[\int_0^\infty \int_{\mathbb{R}} \Bigg\{\sum_{i=1}^N r_i \sqrt{b(s_i)}\,\phi\left(z; \frac{A(s_i)}{\sqrt{2}}, \frac{a(s_i)}{4w}\right)\Bigg\}^2 \mathrm{d}z\, w^{-1/2}\,\mathrm{d}F(w)\Bigg] \geq 0.$$

References

Alegría, A., Emery, X., Filosi, T., and Porcu, E. (2026). Computationally efficient algorithms for simulating isotropic Gaussian random fields on graphs with Euclidean edges. *Journal of Computational and Graphical Statistics*, 35(2):937–950.

Statistica Sinica: Newly accepted Paper

REFERENCES

Anderes, E., Møller, J., and Rasmussen, J. G. (2020). Isotropic covariance functions on graphs and their edges. *The Annals of Statistics*, 48(4):2478–2503.

Anderes, E. B. and Stein, M. L. (2011). Local likelihood estimation for nonstationary random fields. *Journal of Multivariate Analysis*, 102(3):506–520.

Baddeley, A., Nair, G., Rakshit, S., and McSwiggan, G. (2017). "stationary" point processes are uncommon on linear networks. *Stat*, 6(1):68–78.

Baddeley, A., Nair, G., Rakshit, S., McSwiggan, G., and Davies, T. M. (2021). Analysing point patterns on networks—A review. *Spatial Statistics*, 42:100435.

Baddeley, A. and Turner, R. (2005). Spatstat: an r package for analyzing spatial point patterns. *Journal of statistical software*, 12:1–42.

Bolin, D., Riera-Segura, L., and Simas, A. B. (2025). A new class of non-stationary gaussian fields with general smoothness on metric graphs. *arXiv preprint arXiv:2501.11738*.

Bolin, D., Simas, A. B., and Wallin, J. (2024). Gaussian Whittle–Matérn fields on metric graphs. *Bernoulli*, 30(2):1611–1639.

Chang, Y.-M., Hsu, N.-J., and Huang, H.-C. (2010). Semiparametric estimation and selection for nonstationary spatial covariance functions. *Journal of Computational and Graphical Statistics*, 19(1):117–139.

Cox, D. R. (1955). Some statistical methods connected with series of events. *Journal of the Royal Statistical Society: Series B (Methodological)*, 17(2):129–157.

Statistica Sinica: Newly accepted Paper

REFERENCES

Cronie, O., Moradi, M., and Mateu, J. (2020). Inhomogeneous higher-order summary statistics for point processes on linear networks. *Statistics and Computing*, 30(5):1221–1239.

Dahlhaus, R. (1997). Fitting time series models to nonstationary processes. *The Annals of Statistics*, 25(1):1–37.

Dvořák, J., Møller, J., Mrkvička, T., and Soubeyrand, S. (2019). Quick inference for log Gaussian Cox processes with non-stationary underlying random fields. *Spatial Statistics*, 33:100388.

Erdélyi, A. (1954). *Tables of Integral Transforms, Volume II.* McGraw-Hill, New York.

Filosi, T., Agostinelli, C., and Porcu, E. (2027). Temporally-evolving generalised networks and their kernels. *Statistica Sinica (forthcoming)*.

Filosi, T., Porcu, E., Emery, X., Agostinelli, C., and Alegría, A. (2025). Vector-valued Gaussian processes and their kernels on a class of metric graphs. *arXiv preprint arXiv:2501.10208*.

González-Pérez, I., Borrajo, M. I., and González-Manteiga, W. (2025). Nonparametric testing of first-order structure in point processes on linear networks. *Statistical Papers*, 66(2):42.

Kidd, B. and Katzfuss, M. (2022). Bayesian nonstationary and nonparametric covariance estimation for large spatial data (with discussion). *Bayesian Analysis*, 17(1):291–351.

Kleiber, W. and Nychka, D. (2012). Nonstationary modeling for multivariate spatial processes. *Journal of Multivariate Analysis*, 112:76–91.

Klein, D. and Randić, M. (1993). Resistance distance. *Journal of Mathematical Chemistry*,

Statistica Sinica: Newly accepted Paper

12:81–95.

Koumandos, S. and Pedersen, H. L. (2019). On generalized Stieltjes functions. *Constructive Approximation*, 50(1):129–144.

Liang, M. and Marcotte, D. (2016). A class of non-stationary covariance functions with compact support. *Stochastic Environmental Research and Risk Assessment*, 30(3):973–987.

Mateu, J., Fernández-Avilés, G., and Montero, J. M. (2013). On a class of non-stationary, compactly supported spatial covariance functions. *Stochastic Environmental Research and Risk Assessment*, 27(2):297–309.

Menegatto, V. (2020). Positive definite functions on products of metric spaces via generalized Stieltjes functions. *Proceedings of the American Mathematical Society*, 148(11):4781–4795.

Møller, J. and Rasmussen, J. G. (2024). Cox processes driven by transformed Gaussian processes on linear networks—A review and new contributions. *Scandinavian Journal of Statistics*, 51(3):1288–1322.

Moradi, M. and Mateu, J. (2020). First-and second-order characteristics of spatio-temporal point processes on linear networks. *Journal of Computational and Graphical Statistics*, 29(3):432–443.

Moradi, M. and Sharifi, A. (2024). Summary statistics for spatio-temporal point processes on linear networks. *Spatial Statistics*, 61:100840.

Paciorek, C. J. (2003). *Nonstationary Gaussian processes for regression and spatial modeling.*

Statistica Sinica: Newly accepted Paper

Ph.D. thesis, Carnegie Mellon University.

Paciorek, C. J. and Schervish, M. J. (2006). Spatial modelling using a new class of nonstationary covariance functions. *Environmetrics*, 17(5):483–506.

Porcu, E., White, P. A., and Genton, M. G. (2023). Stationary nonseparable space-time covariance functions on networks. *Journal of the Royal Statistical Society Series B: Statistical Methodology*, 85(5):1417–1440.

Schmidt, A. M. and Guttorp, P. (2020). Flexible spatial covariance functions. *Spatial Statistics*, 37:100416.

Ver Hoef, J. M. and Peterson, E. E. (2010). A moving average approach for spatial statistical models of stream networks. *Journal of the American Statistical Association*, 105(489):6–18.

Voss, S. C., Main, B. Y., and Dadour, I. R. (2007). Habitat preferences of the urban wall spider oecobius navus (araneae, oecobiidae). *Australian Journal of Entomology*, 46(4):261–268.

Yaglom, A. M. (1987). *Correlation theory of stationary and related random functions, Volume I: Basic results*, volume 1. Springer.

Department of Statistics, Pontificia Universidad Católica de Chile, Santiago, Chile.

E-mail: alfredo.alegria@uc.cl